NMR Determination of the Fractal Dimension in Silica Aerogels

F. Devreux, J. P. Boilot, F. Chaput, and B. Sapoval
Laboratoire de Physique de la Matière Condensée, Ecole Polytechnique, 91128 Palaiseau CEDEX, France
(Received 9 February 1990)

^{29}Si nuclear relaxation experiments were performed in different forms of silica (alcogel, aerogel, amorphous, and crystallized) doped with paramagnetic impurities. Magic-angle spinning is used to quench the nuclear-spin diffusion. Under this condition, the saturation recovery of the ^{29}Si magnetization follows a power law in a very large time range (up to 5 orders of magnitude). This nonexponential relaxation $m(t)\sim t^{\alpha}$ reflects the mass distribution in the sample: $M(r)\sim r^{D}$ with $\alpha=D/6$. In aerogels, the measured fractal dimension $D\approx 2.2$ is in agreement with that determined by small-angle x-ray scattering. In densified materials, a dimension $D\approx 3$ is actually observed.

PACS numbers: 61.42.+h, 76.60.Es

So far, small-angle scattering techniques have been the most popular method to characterize the geometrical arrangement of microscopic objects displaying self-similar or fractal structure. In the present Letter, a new method is proposed and worked out: It is based upon the nuclear relaxation induced by paramagnetic impurities diluted in a fractal lattice. Contrary to the scattering techniques which involve an analysis of the scattered intensity in reciprocal space, the present method gives directly the mass-to-distance relation in real space: $M(r)\sim r^{D}$, with D being the fractal dimension. If a saturation comb is applied to kill the spin magnetization of nuclei belonging to the lattice backbone, the recovery of this magnetization will reflect the spatial repartition of the nuclear spins which relax to their equilibrium polarization by dipolar flipping with the dilute magnetic ions. Since the time constant for the dipolar coupling relaxation increases with the distance as r^{6}, the recovered magnetization at time t after saturation will be that of the spins that are contained in a sphere of radius $r\sim t^{1/6}$, and therefore it will show a time dependence of $m(t)\sim t^{D/6}$. Such a nonexponential behavior is expected and was observed, thirty years ago, in dense materials, where it gives rise to a square-root law: $m(t)\sim\sqrt{t}$.[1] On the other hand, energy migration processes have already been considered as a possible method to determine the fractal dimension.[2] For example, a dimension $D=1.74$ was found in porous Vycor glass[3] by observing the luminescence decay of optically excited donors by dipole-dipole coupling with acceptor molecules.

The systems which have been chosen for this study are silica aerogels, which are expected to present fractal characteristics.[4,5] They are obtained by sol-gel condensation in the acidic medium of a silicon alkoxyde, tetraethoxysilane.[6] Chromium nitrate is added in the polymerization solution as an NMR relaxing agent. The alcogel, which results from the gelation of this solution, consists of an interconnected network of branched polymers in which solvent molecules are embedded. By evacuating the solvent under hypercritical conditions ($T=255\,^{\circ}$C and $p=75$ bars), an aerogel is obtained, whose density (0.17 g/cm^3 in the present case) is controlled by the monomer concentration in the initial solution. Then, the aerogels can be sintered. Heating at 1000 °C leads to an amorphous material whose density is about 1.6 g/cm^3 and heating above 1200 °C gives the cristobalite phase of the silica with a density of 2.3 g/cm^3.

^{29}Si NMR measurements have been performed at 71.4 MHz using a Bruker MSL 360 spectrometer and a Doty magic-angle-spinning (MAS) probe. Figure 1 shows the spectra of the different forms of silica. In the alcogel and in the aerogel, three broad lines are observed, which correspond to silicon nuclei having two, three, and four siloxane bridges. This reflects the lacunar structure of

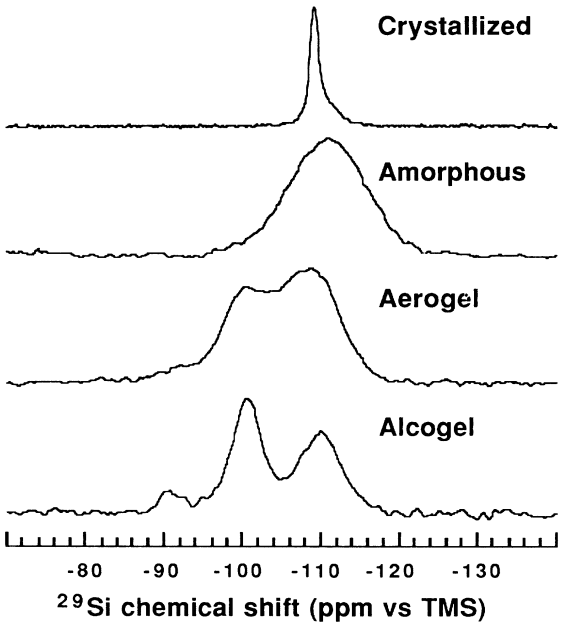

FIG. 1. ^{29}Si MAS NMR spectra for different forms of silica.

these systems. In the densified materials, there only remains the line due to four-coordinated silicon. As a result of the random or ordered environment of the silicon atoms, the line is broad for the amorphous compound and sharp for the crystallized one.

Figure 2 shows the recovery of the ^{29}Si magnetization in five compounds: an alcogel, two aerogels with different paramagnetic impurity concentrations, and an amorphous and a crystallized sample. The chromium to silicon ratio in the polymerization solution was 6×10^{-3} for all the samples, except for the second aerogel for which it was 6×10^{-4}. The saturation was achieved by a comb of twenty to thirty $\pi/2$ pulses (pulse duration 3 μs). Then the free-induction decay was recorded after a variable delay ranging from 100 ms to 70000 s. Because of the very large time scale involved, the number of accumulations was varied to save acquisition time: from several thousand for the shortest delay times when the signal is weak to a few (1–4) for the longest times when the whole magnetization of the sample is recovered. Magnetization was measured by taking either the area or the amplitude of the Fourier transform spectra. Both methods give identical time dependence, although the amplitude data (shown in Fig. 2) are less scattered.

The relaxation is strongly nonexponential for all the samples studied. From the log-log plot in Fig. 2, it turns out that the time dependence of the magnetization recovery follows a power law $m(t)\sim t^{\alpha}$ in an extended time range, before reaching a saturation plateau. It is quite unusual to observe a power law for such a long time range, because the direct dipolar coupling between nuclear and electronic spins is generally relayed at long distances by nuclear-spin diffusion, which gives rise to an exponential recovery.[1] This short cut is avoided in the present experiment by magic-angle spinning which averages the secular part of the dipolar coupling between nuclear spins. This inhibits the flip-flop transitions between neighboring ^{29}Si and quenches the nuclear-spin diffusion process.

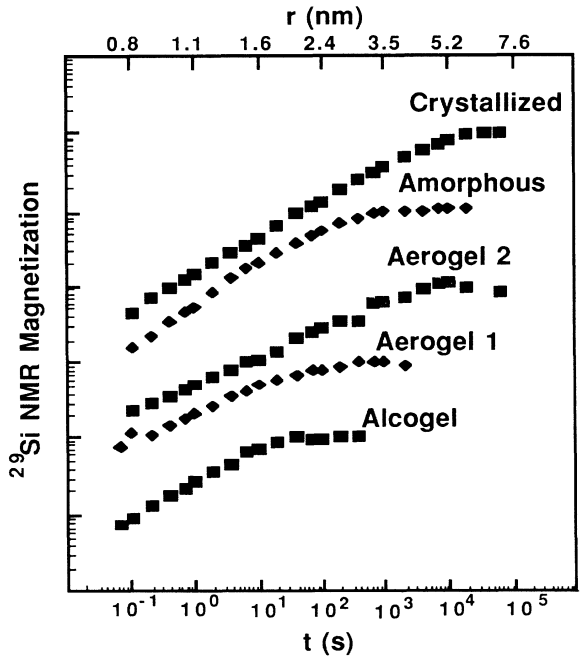

FIG. 2. Time dependence of the ^{29}Si magnetization saturation recovery for different forms of silica. The upper scale is labeled in distance units according to $r=(At)^{1/6}$ with $A=2.0$ nm^6/s. The curves are arbitrarily shifted in the vertical direction.

The ^{29}Si nuclear relaxation rate induced by direct dipolar coupling with a fixed paramagnetic impurity located at a distance r can be expressed as $1/T_{1n}(r)=A/r^6$ with the constant A given by[7]

$$A=\tfrac{1}{15}S(S+1)(h\gamma_n\gamma_e)^2 \times[f(\omega_e-\omega_n)+3f(\omega_n)+6f(\omega_e+\omega_n)], \quad (1)$$

where γ_n and γ_e are the nuclear and electronic gyromagnetic ratios, ω_n and ω_e the nuclear and electronic Larmor frequencies, S the electronic spin ($S=\frac{3}{2}$ for Cr^{3+}), and $f(\omega)$ the spectral density. As both nuclear and electronic spins are fixed, the only source of local field fluctuations is the electronic-spin relaxation and the spectral density can be taken as $f(\omega)=2T_{1e}/[1+(\omega T_{1e})^2]$, where T_{1e} is the electronic relaxation time. In Eq. (1), an angular averaging of the dipolar interactions has been performed on the orientations of the vector **r** joining the nuclear and electronic spins. Moreover, it can be shown that this expression, which was established in the static case, remains valid under MAS conditions provided that the rotation frequency ω_r can be neglected with respect to ω_n and ω_e.[8] Then the magnetization at time t after saturation is given by[1]

$$m(t)=c\int_{r_m}^{r_M}[1-\exp(-At/r^6)]\mu_0(r)dr, \quad (2)$$

where c is the electronic spin concentration, $dm_0(r)=\mu_0(r)dr$ is the equilibrium ^{29}Si magnetization within a small slice at a distance r from an electronic spin, and r_m and r_M are short- and long-range cutoffs, to be discussed below. Between these two cutoffs, Eq. (2) can be approximated by replacing the exponential term by a Heaviside function, leading to $m(t)\approx cm_0(r=(At)^{1/6})$. Taking into account that the equilibrium magnetization is proportional to the mass and therefore has the same variation as a function of the distance [$m_0(r)\sim r^D$], the announced time dependence, $m(t)\sim c(At)^{\alpha}$ with $\alpha=D/6$, is obtained.

The values of the exponent α are obtained by fitting the power-law regimes in Fig. 2 up to the point where the magnetization is half of its saturation value. The resulting values for $D=6\alpha$ are listed in Table I. Finding values near $D=3$ for the densified materials is quite satisfactory and provides a good reliability test. For the alcogel and the aerogel, the NMR results can be compared

TABLE I. Experimental data for the five silica compounds studied: D is the dimension as determined by NMR or SAXS techniques. c is the electronic-spin to silicon-atom ratio, as measured by EPR (except for the alcogel and the second aerogel for which the chromium concentration in the polymerization solution is given), and r_M is the corresponding mean distance between electronic spins.

	D (NMR)	D (SAXS)	c	r_M (nm)
Alcogel	2.85	2.0	6×10^{-3}	1.4
Aerogel 1	2.3	2.3	5×10^{-3}	2.5
Aerogel 2	2.1	2.3	6×10^{-4}	6.4
Amorphous	3.1	Dense	3×10^{-4}	3.7
Crystallized	2.85	Dense	9×10^{-5}	5.6

to those of small-angle x-ray-scattering (SAXS) experiments performed on the same samples. The data in Fig. 3 show the scattered intensity $I(Q)$ as a function of the scattering vector amplitude. These data are fitted with a theoretical expression describing the scattering by fractal objects with limited correlation length.[9] From this fit, independent determinations of the fractal dimension were obtained which are also reported in Table I. They turn out to be in good agreement with the NMR results for the aerogel and in noticeable disagreement for the alcogel. This is easily explained by remarking that the relation $m_0(r)\sim r^D$, from which the NMR D is deduced, describes the mass distribution around the magnetic impurities. Since the chromium spins can be everywhere in the alcogel solution, the NMR relaxation no longer reflects the spatial correlations on the silica polymer, but the mass repartition in the gelled solution. As the latter has no reason to be different from a regular tridimensional distribution, it is quite consistent to obtain by NMR a value near $D=3$ for this sample.

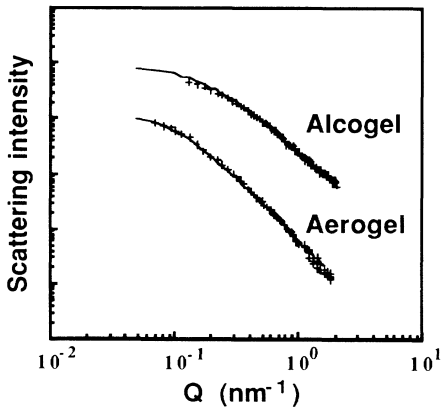

FIG. 3. Small-angle x-ray-scattering curves in silica alcogel and aerogel. The continuous lines are the results of fits by Eq. (16) of Ref. 9. The parameters of the fit are the fractal dimension ($D=2.0$ for the alcogel and $D=2.3$ for the aerogel), the correlation length ($\xi=6.5$ nm for the alcogel and $\xi=9.0$ nm for the aerogel), and the size of the elementary particles from which the fractal clusters are grown ($a_0=0.5$ nm for both samples).

EPR experiments have been performed in the first aerogel and in the two densified materials to measure the spin concentration and the electronic T_{1e}. The values of the EPR spin concentration expressed in terms of electronic-spin to silicon-atom ratio are listed in Table I. For the aerogel, it is in agreement within 15% with the value in the polymerization solution. In densified materials, the spin concentration is much smaller: This is probably due to the formation of segregated microcrystals of antiferromagnetic Cr_2O_3 during the sintering process. As concerns the electronic relaxation, the impossibility to saturate the EPR lines gives a lower limit: $(T_{1e})^{-1}>5\times10^4\ s^{-1}$, whereas a higher limit is imposed by the EPR linewidth which is about 450 G. In fact, as an extreme narrowing regime is expected in the case of strongly lattice-coupled transition ions, it is not unreasonable to estimate tentatively the relaxation rate from the linewidth by taking $(T_{1e})^{-1}=(T_{2e})^{-1}=7\times10^9\ s^{-1}$. With this value, the constant A defined in Eq. (1) can be evaluated as $A=2.0\ nm^6/s$. This establishes the time-to-distance relation, i.e., $r=(At)^{1/6}$, which is not very sensitive to the precise value of A. Thus, the horizontal axis in Fig. 2 can be labeled in distance units (upper scale), and this allows a direct visualization of the growth of the relaxed regions. It turns out that the distance range explored corresponds to the length scale over which the alcogel and the aerogels are expected to be fractals.

The short-distance cutoff in Eq. (2) is due to the fact that ^{29}Si nuclear spins that are too close to an electronic spin feel a large dipolar field, which puts them out of the NMR line and makes them unobservable. Usually, this corresponds to the distance at which the electronic dipolar shift $\delta\omega_{dip}$ is equal to the NMR linewidth.[1] However, in the present case, the secular part of this dipolar coupling, which is responsible for the NMR line shift, can be averaged to zero by the magic-angle spinning and the condition becomes $\delta\omega_{dip}(r_m)\approx\omega_r$. Thus, expressing the typical size of the paramagnetic dipolar shift as

$$\delta\omega_{dip}(r)=\tfrac{1}{6}\,\omega_n S(S+1)(h\gamma_e)^2/kTr^3, \qquad (3)$$

one obtains $r_m\approx0.4$ nm for a rotation frequency $\omega_r=3\times10^4\ s^{-1}$. This corresponds to times shorter than those that appear in Fig. 2. Measurements performed at very short times give small noisy signals that are dephased with respect to those at larger times. This dephasing should reflect the line distortion due to the presence of a large local magnetic field.

Finally, the long-range cutoff corresponds to the distance at which the volumes relaxed by different paramagnetic centers overlap. It an be estimated from the impurity concentration by the relation $c=(r_0/r_M)^D$, where $r_0\approx0.25$ nm is the distance between two neighboring silicon atoms. The values of r_M corresponding to

the different samples are listed in Table I. They are in quite good agreement with the points at which the time dependence of the magnetization enters the saturation regime in Fig. 2. Whereas the scaling of these points with c in different samples is not surprising, obtaining consistent values of r_M actually corroborates the length scale which has been deduced from the evaluation of the constant A.

In conclusion, the present method allows us to explore the geometry of fractal systems in real space at microscopic scale. It has been successfully applied to silica aerogels by using ^{29}Si NMR, taking advantage of the quenching of the nuclear-spin diffusion by magic-angle spinning. However, it can be remarked that there are two additional effects that strongly depress the nuclear-spin diffusion in these kinds of systems. First, the fractal geometry imposes a tortuous path to the magnetization leading to a slow anomalous diffusion, and second, the structural disorder may cause considerable shifts of the NMR lines of neighboring spins making the dipolar flipping quite inefficient. On the other hand, the poor signal-to-noise ratio related to this rare spin system leads to very long accumulation times and limits the accuracy of the fractal-dimension determination. To avoid this drawback, it might be advantageous to extend the method to abundant nuclei, such as protons, provided that their dipolar interactions are suppressed by appropriate multipulse techniques.[10,11]

SAXS measurements by A. Lecomte and A. Dauger are warmly acknowledged. The Laboratoire de Physique de la Matière Condensée is supported by the Centre National de la Recherche Scientifique as Unité de Recherche Associée No. 1254. One of us (F.D.) is also a member of the Service de Physique, Centre d'Etudes Nucléaires de Grenoble, France.

[1]W. E. Blumberg, Phys. Rev. **119**, 79 (1960).

[2]P. Evesque, in *The Fractal Approach to Heterogeneous Chemistry,* edited by D. Avnir (Wiley, New York, 1989).

[3]U. Even, K. Rademann, J. Jortner, N. Manor, and R. Reisfeld, Phys. Rev. Lett. **52**, 2164 (1984).

[4]D. W. Schaefer and K. D. Keefer, Phys. Rev. Lett. **56**, 2199 (1986).

[5]R. Vacher, T. Woignier, J. Pelous, and E. Courtens, Phys. Rev. B **37**, 6500 (1988).

[6]J. C. Pouxviel, J. P. Boilot, J. C. Beloeil, and J. Y. Lallemand, J. Non-Cryst. Solids **89**, 345 (1987).

[7]A. Abragam, *The Principles of Nuclear Magnetism* (Oxford Univ. Press, New York, 1961), Chaps. VIII and IX.

[8]U. Haeberlin and J. S. Waugh, Phys. Rev. **185**, 420 (1969).

[9]J. Texeira, J. Appl. Cryst. **21**, 781 (1988).

[10]D. Tse and S. R. Hartmann, Phys. Rev. Lett. **21**, 511 (1968).

[11]M. Mehring, *High Resolution NMR in Solids* (Springer-Verlag, Berlin, 1983), Chap. 8.